Identification of Novel Mutation Sites in DNAH1 of Multiple Morphological Anomalies of the Flagella Patients

Xiong Wang
Reproductive Medicine Center, Affiliated Yantai Yuhuangding Hospital of Qingdao University, 20 Yuhuangding East Road, Yantai, Shandong, 264000, China
Yan-Wei Sha
Andrology, Xiamen Maternity and Child Care Hospital, Xiamen, Fujian 361005, China
Xing-shen Zhu
School of Pharmaceutical Sciences, Xiamen University, Xiamen, Fujian 361005, China
Xiao-ya Zhang
Xiamen University
Yuan-qing Cui
Reproductive Medicine Center, Affiliated Yantai Yuhuangding Hospital of Qingdao University, 20 Yuhuangding East Road, Yantai, Shandong, 264000, China
Jie Chen
Reproductive Medicine Center, Affiliated Yantai Yuhuangding Hospital of Qingdao University, 20 Yuhuangding East Road, Yantai, Shandong, 264000, China
Hua-yu Lian
Reproductive Medicine Center, Affiliated Yantai Yuhuangding Hospital of Qingdao University, 20 Yuhuangding East Road, Yantai, Shandong, 264000, China
Wei Yan
Reproductive Medicine Center, Affiliated Yantai Yuhuangding Hospital of Qingdao University, 20 Yuhuangding East Road, Yantai, Shandong, 264000, China
He-jia Yuan
Reproductive Medicine Center, Affiliated Yantai Yuhuangding Hospital of Qingdao University, 20 Yuhuangding East Road, Yantai, Shandong, 264000, China
Wei-bing Qin
NHC Key Laboratory of Male Reproduction and Genetics (Family Planning Research Institute of Guangdong Province, Guangzhou 510600, China
Yunge Tang
NHC Key Laboratory of Male Reproduction and Genetics (Family Planning Research Institute of Guangdong Province, Guangzhou 510600, China
Xin-zhong Zhang
NHC Key Laboratory of Male Reproduction and Genetics (Family Planning Research Institute of Guangdong Province, Guangzhou 510600, China
Huiliang Zhou
Department of Andrology, First Affiliated Hospital of Fujian Medical University, Fuzhou, Fujian, China
Zhongxian Lu (zhongxian@xmu.edu.cn)
School of Pharmaceutical Sciences, Xiamen University, Xiamen, Fujian 361005, China https://orcid.org/0000-0002-1682-7147

Research article

Keywords: MMAF, infertility, WES, DNAH1, ICSI

Posted Date: March 8th, 2021

DOI: https://doi.org/10.21203/rs.3.rs-279593/v1

Abstract

Background

Multiple morphological anomalies of the sperm flagella (MMAF) is a term used to describe abnormalities in sperm morphology, which lead to primary infertility in males. Intracytoplasmic sperm injection (ICSI) is an effective treatment for MMAF. However, ICSI failure rates remain high in MMAF patients. Our purpose was to investigate novel gene mutations in a cohort of nineteen patients with MMAF and assess the impact of these mutations on assisted reproductive therapy.

Methods

We recruited nineteen infertile patients with MMAF and twenty healthy men with proven fertility at the Affiliated Yantai Yuhuangding Hospital of Qingdao University. The morphology of the spermatozoa was observed using Papanicolaou staining and the ultrastructure of the spermatozoa was inspected using transmission electron microscopy. Gene mutations were evaluated using whole-exome sequencing and novel mutations were further validated in patients and their parents using Sanger sequencing. The effect of these novel mutation sites on the expression of DNAH1 was analysed using immunofluorescence, and the effect of these novel mutations on pregnancy outcome was analysed using intracytoplasmic sperm injection (ICSI).

Results

Spermatozoa from 19 patients presented with a typical MMAF phenotype including severe ultrastructural defects. We identified ten novel mutation sites in the *DNAH1* locus from six of these patients, none of which were identified in *DNAH1* or the other MMAF-related genes from the twenty men with proven fertility. In the sperm from these patients, DNAH1 was absent. Three patients with *DNAH1* mutation who underwent intracytoplasmic sperm injection (ICSI) had a good outcome.

Conclusion

Here, we describe several novel compound heterozygous mutations and a novel homozygous mutation in *DNAH1* from six independent MMAF patients. This study adds to the body of knowledge surrounding the genetic landscape of MMAF and *DNAH1* improving our ability to diagnose and treat MMAF efficiently.

Background

Male infertility affects approximately 7% of men worldwide [1]. Multiple morphological anomalies of the flagella (MMAF) is characterised by several morphological defects in sperm flagella, including absent, short, bent, coiled, and/or irregular flagella [3]. MMAF is a rare version of asthenozoospermia with serious consequences for male fertility.

Genetic defects are a common cause of male infertility, accounting for up to 15% of cases [2]. Following the development of next-generation sequencing (NGS) technology, sequencing of whole-exomes has been widely applied to detect pathogenic variants in MMAF patients [3, 4]. A large number of mutated genes related to MMAF have been reported in the past few years, including *DNAH1* [3, 5-7], *DNAH2* [8], *DNAH8* [9, 10], *AKAP4* [11], *CCDC39* [12], *CFAP43* and *CFAP44* [13-15], *CFAP58* [16], *CFAP69* [17], *CEP135* [18], *WDR66* [20-22], *FISP2* [19], *ARMC2* [23], *SPEF2* [24-26] and *DNAH17* [27, 28]. Of these, mutations in *DNAH17* are the most prevalent and result However, further investigations are necessary to fully elucidate the genetic defects in patients with MMAF.

Patients with MMAF have highly deformed sperm, often accompanied by severe asthenozoospermia, making it difficult for them to conceive spontaneously [29, 30]. Intracytoplasmic sperm injection (ICSI) is an effective treatment for MMAF, which has been shown to achieve solid outcomes in patients with mutations in *DNAH1*, *DNAH2*, *DNAH8*, *WDR19*, *CFAP74*, *CFAP43*, and *CFAP44* [8, 10, 31-34]. However, there are several MMAF patients who have tried ICSI multiple times and remain unable to conceive [18, 35]. Therefore, a comprehensive catalogue of the MMAF disease-causing variants will enable patients with MMAF to benefit from genetic diagnosis and the assessment for *in vitro* fertilisation outcomes.

In this study, we recruited a cohort of nineteen MMAF patients and identified ten novel mutation sites within *DNAH1*. Our findings enrich the mutation spectrum for MMAF and contribute to the clinical diagnosis and therapeutic treatment available for these patients.

Methods

Patients and control subjects

A cohort of nineteen patients with MMAF and their families were recruited for this study from the Affiliated Yantai Yuhuangding Hospital of Qingdao University. Twenty men with proven fertility, who already had at least one child, served as normal controls. The inclusion and exclusion criteria for this study was identical to those used in previously published reports [37]. Physical and andrological hormone examinations were also performed, and all of the selected participants exhibited normal external genitalia, bilateral testicular development, and normal andrological hormone levels. No abnormalities were observed in the bilateral spermatic veins upon palpation, and all patients presented with normal chromosomal karyotypes (46, XY). All participants answered a questionnaire about primary ciliary dyskinesia (PCD) -associated manifestations, including long instances of coughing with phlegm, year-round nasal congestion, chronic sinusitis, bronchiectasis, recurrent lower respiratory tract infections, pneumonia, and otitis media [38]. A total of 5 mL of peripheral blood was collected from each participant for whole genome and Sanger sequencing.

Whole-exome sequencing (WES) and Sanger sequencing validation

Whole-exome sequencing was performed as described previously [39]. The reads were aligned to the UCSC hg19 genome using the Burrows-Wheeler Aligner (http://biobwa.sourceforge.net/) and variants were annotated using ANNOVAR (http://www.openbioinformatics.org/annovar/). Each variant was then evaluated for pathogenicity using Polyphen2 (http://genetics.bwh.harvard.edu/pph2/) and Mutation Taster (http://www.mutationtaster.org/). They were also cross-referenced with the Exome Aggregation Consortium (ExAC) (http://exac.broadinstitute.org/), genome aggregation database (gnomAD, http://gnomad.broadinstitute.org/), 1000 Genomes Project (http://www.1000genomes.org/data), and ESP6500 (http://evs.gs.washington.edu/EVS/) databases for novelty and frequency analysis. Mutations that met these criteria were then assigned as missense, nonsense, frame-shift, or splice site variant and annotated as absent or rare variants. The *DNAH1* mutations were further validated using Sanger sequencing and the primers used for this sequencing are listed in Supplementary Table 2.

Papanicolaou staining

Spermatozoa were examined using Papanicolaou staining in accordance with the World Health Organization standards for human semen examination and processing (5th ed.) with minor modifications to confirm any morphological changes in the sperm tails. Briefly, slides were fixed in 95% ethanol (Xilong, Shantou, China), and then immersed in an alcohol gradient from 80% to 50%. The slides were then rinsed with distilled water, and stained with haematoxylin (Zsbio, Beijing, China). Following this, the slides were dehydrated in an alcohol gradient from 50% to 90%, dyed with Orange G6 (Solarbio, Beijing, China) and EA50 (Solarbio, Beijing, China), and dehydrated again using 95% and 100% alcohol (Xilong, Shantou, China). Finally, the slides were washed in xylene and mounted using a permanent mounting medium.

Transmission electron microscopy (TEM)

Sperm samples were examined via TEM according to a previously published procedure that allows for the evaluation of subcellular structural changes in these samples [25]. Briefly, prepared spermatozoa were immobilised with 2.5% phosphate-buffered glutaraldehyde (Electron Microscopy Sciences, Hatfield, USA), then the samples were washed with 0.1 M phosphate buffer (pH 7.2) and post-fixed with 1% osmium tetroxide (Sigma-Aldrich, St. Louis, USA). Dehydration was performed by sequentially treating samples with an alcohol gradient and 100% acetone (Xilong, Shantou, China) and infiltrated with 1:1 acetone and resin (SPI Supplies, West Chester, USA). After infiltration, the samples were embedded and polymerised. Ultrathin sections (70 nm thick) were cut and collected on 200 mesh TEM copper grids, and then counterstained with uranyl acetate and lead citrate. The ultrastructure of each sample were observed and photographed using a Tecnai G2 Spirit transmission electron microscope (FEI, Oregon, USA) at 80 kV.

Immunostaining of spermatozoa

We performed immunostaining of the spermatozoa as described previously [18]. Briefly, the prepared spermatozoa were smeared onto poly L-lysine-coated slides, allowed to air-dry, washed in phosphate-buffered saline (PBS), fixed in 4% paraformaldehyde (PFA) (Sigma, St. Louis, USA) for 10 min at room temperature, and washed twice with PBS. Next, the samples were permeabilised using 0.2% Triton X-100 (Sigma, St. Louis, USA) and blocked for 30 min at room temperature. Slides were incubated with primary antibodies for 1 h at room temperature and then with secondary antibodies for 1 h at RT. Samples were subsequently washed three times with PBS and mounted using Vectorshield supplemented with DAPI (Vector Laboratories, Burlingame, USA), and examined under a laser scanning confocal immunofluorescence microscope (Carl Zeiss, Jena, Germany). The specific antibodies used in these assays are listed in Supplementary Table 3.

Ovarian stimulation, intracytoplasmic sperm injection, and embryo transfer

Ovulation was triggered in the wives of the patients using the long standard ovarian stimulation protocol. Briefly, women were given 75 IU Recombinant Follitropin Beta Injection (Merck Sharp & Dohme, Kenilworth, USA) and 75 IU human menopausal gonadotropin (Ferring Pharmaceuticals, Saint Prex, Switzerland), and their follicular response was evaluated after 5 days of gonadotrophin stimulation. Ultrasound was used to monitor the diameter of the follicles and when at least two follicles were ≥18 mm in diameter, patients received 6500 or 10 000 IU human chorionic gonadotropin (Livzon, Zhuhai, China). We retrieved oocytes 34–36 h later using vaginal ultrasound-guided follicular puncture.

The intracytoplasmic sperm injection (ICSI) procedure was performed as previously described [40]. Briefly, 18–19 h after fertilisation, samples were evaluated for the presence of two pronuclei and two polar bodies with fertilised oocytes individually cultured in G1 medium (Vitrolife, Västra Frölunda, Swedish) until the day of transfer, which was performed 48–72 h after oocyte retrieval. Cleaving embryos were evaluated for cell number, blastomere appearance, and fragmentation rate. The best embryos were selected for transfer, and additional high-quality embryos were frozen. Two embryos from each couple were transferred using ultrasound guidance and patients received luteal support, including 600 mg of vaginally administered micronised progesterone (Besins Healthcare, Gabian, Monaco). Serum hCG levels were measured 14 days after embryo transfer and clinical pregnancy was defined as the presence of a visible sac and foetal heartbeat 7 weeks after embryo transfer.

Results

Identification of novel *DNAH1* mutation sites in MMAF patients

A cohort of nineteen patients was recruited for this study and none of these patients presented with any clinical symptoms of PCD. Genomic DNA was extracted from the whole blood of each MMAF patient and subjected to WES in an effort to identify novel chromosomal mutations. After excluding the sense and non-pathogenic mutations, using bioinformatics analysis, we identified several rare and potentially pathogenic mutations in each of these nineteen patients. The list of the rare and potentially pathogenic mutations in the six patients harbouring *DNAH1* mutations are summarised in Supplemental Tables 5–10. However, among these sites, only *DNAH1* was closely associated with flagellar function and both homozygous and compound heterozygous mutations in *DNAH1* were identified in eight of the patients (42.1% of 19 total, Supplementary Table 4) in this study. Two known mutations for known homozygous

mutation sites, g.52430998-52430999del (p.Pro3909fs) in patients P007 and P016 (from different consanguineous families) and ten novel mutation sites in *DNAH1* from six patients (P002, P005, P008, P011, P015, and P017) were identified in this study (Fig. 1A). The physical examination indices of the six patients harbouring novel mutations of *DNAH1* are summarised in Supplementary Table 1 and the semen characteristics of these patients are described in Table 1.

The mutation sites in *DNAH1* were further validated in both the patients and their parents using Sanger sequencing. The rectangles indicate each of the mutation sites identified in the six sterile patients with the red rectangles identifying the ten novel mutations. With the exception of P017, who has a younger brother, all of the other sterile patients came from one-child families. A novel homozygous mutation, g.52390782C>G (p.Tyr1282X), was identified in P011 whose parents both carried a heterozygous g.52390782C>G (p.Tyr1282X) mutation (Fig. 1A, F011). Compound heterozygous mutations were identified in each of the remaining patients and can be described as follows: g.52400764G>C (p.Ala1876Pro) and g.52431052G>A (p.Asp3927Asn) in P002 (Fig. 1A, F002); g.52414014C>A (p.Gln2491Lys) and g.52423486C>T (p.Arg3169Cys) in P005 (Fig. 1A, F005); g.52417875G>C (3p21.1) and g.52430998_52430999del (p.Pro3909fs) in P008 (Fig. 1A, F008); g.52370722_52370723 del (p.Thr2141fs) and g.52375320C>T (p.Arg2356Trp) in P015 (Fig. 1A, F015); and g.52417883G>A (p.Gly2720Arg) and g.52432907A>T (p.Asp4044Val) in P017 (Fig. 1A, F017). The g.52430998_52430999del (p.Pro3909fs) mutations have been previously described; however, the other ten mutation sites are all novel for MMAF. All these mutations were segregated by family, with each parent carrying one mutation site (Fig. 1A).

All of these mutant sites are located in important regions of *DNAH1* (Fig. 1B), including exons or splice sites while the amino acid substitutions primarily occur in the functional domains of the DNAH1 protein (Fig. 1C). The sites of these mutations indicate that they could affect the function of DNAH1. Furthermore, the impact of these mutations on protein function was supported by bioinformatics analysis, which was performed using the Polyphen2_HDIV, Polyphen-2_HVAR, LRT, Mutation Taster, FATHMM_MKL, GenoCanyon, and ClinPred databases (Table 2). Most of the mutation sites were highly conserved, as predicted by the GERP++, phyloP, phastCons, and SiPhy databases (Table 3). The frequency of the observed mutations in the general population was also assessed using the 1000 Genomes, ESP6500, and gnomAD databases, and the results showed that these are rare mutation sites (Table 3). The location, pathogenicity, conservation rates and rarity of these *DNAH1* mutations suggest that these mutations may be the primary cause of MMAF in these patients.

Phenotypes of patients with *DNAH1* mutations

Sperm samples from each of the six patients with *DNAH1* mutations and MMAF all presented with low sperm motility (< 5.6%) with between 90% and 100% of sperm flagella exhibiting morphological anomalies (Table 1). Papanicolaou staining was used to demonstrate the presence of several unique abnormal flagella morphologies in each of these patients (Fig. 2A, indicated by the black arrows). The differences between normal flagella (a) and the typical MMAF phenotypes, including absent (b), short (c), bent (d), coiled (e), and/or irregular flagella (f) as described in Fig. 2B. No obvious lung defects (such as bronchitis or pneumonia) nor heart abnormalities were identified in the chest X-ray images of patients with *DNAH1* mutations (data not available for P015, who refused to receive an X-ray) (Supplementary Fig. 1).

Numerous ultrastructural defects in the sperm flagella were identified in the spermatozoa from patients with *DNAH1* mutations. The normal spermatozoa had an intact midpiece (green arrow) and a principal piece (yellow arrow) in the longitudinal section (Fig. 3A, left). However, most of the sperm flagella in P002 (Fig. 3A, middle) and P005 (Fig. 3A, right) were short (midpiece only, green arrow) or absent (blue arrow). The cross-section at the midpiece showed the typical “9 + 2” microtubule structure in spermatozoa from the control subjects, including nine ODFs, nine DMTs, and a pair of central microtubules (Fig. 3B, left) while the cross-section at the midpiece from P002 revealed the absence of the central pairs (indicated by the red *) and defects in the mitochondrial sheath (indicated by the green #) in these samples (Fig. 3B, middle). The cross-section of the midpiece from P005 showed the complete absence of central pairs (indicated by the red *) and disruption of the mitochondrial sheath (indicated by the green #) (Fig. 3B, right). Spermatozoa from the other four patients with novel *DNAH1* mutation sites showed similar flagellar defects.

Detection of DNAH1 levels in the sperm from patients with *DNAH1* mutations

To assess the influence of these novel mutations on *DNAH1* expression we evaluated the DNAH1 activity in the spermatozoa from these patients using immunofluorescence. Immunofluorescence staining showed that DNAH1 was primarily expressed in the flagella of the normal spermatozoa, but was not observed in the malformed spermatozoa from the patients (Fig. 4).

ICSI outcomes

Three couples (P002, P008, and P011) received reproductive therapy. After ovarian stimulation cycles, we collected oocytes from couples P002, P008, and P011. Subsequently, metaphase II oocytes were injected with the spermatozoa from the patients and two high-quality embryos at the cleavage stage were transferred to the uterus of their respective wives. Any additional high-quality embryos were stored at an ultralow temperature in liquid nitrogen. Fortunately, all the women became pregnant and gave birth (Table 4). The morphological images of the embryogenesis for the implanted embryos are shown in Fig. 5.

Discussion

In this study, we identified eight biallelic mutations (six novel mutations) of *DNAH1* from nineteen sterile patients with MMAF. The known homozygous mutation sites, g.52430998_52430999del (p. Pro3909fs) were identified in patients P007 and P016, who come from different consanguineous families. The mutation in exon 73: g.52430998_52430999del (p.Pro3909fs) in P008 has been reported to induce a frameshift mutation [3, 6, 7] while the other ten mutations are unique to this study and their pathogenic effects are unknown. The mutation in exon 73:g.52370722_52370723del (p.Thr2141fs) may induce a frameshift mutation and produce truncated proteins while the mutation in intron 51: g.52417875G>C (3p21.1) from P008 may affect the final G nucleotide of *DNAH1* intron 51, one of the consensus splice acceptor nucleotides, resulting in abnormal splicing and mRNA degradation by nonsense-mediated mRNA decay (NMD). The mutation in exon 22: g.52390782C>G (p.Tyr1282X) from P011 may introduce a stop codon, resulting in a truncated protein while the other

seven novel mutation sites all occur in exons and may result in a range of changes to the amino acid properties, including side-chain types, acidic alkalinity, charge, and polarity of this protein. We observed that DNAH1 protein was completely absent in the patients' spermatozoa, which suggests that these novel mutations affect the steady-state levels of DNAH1 and eventually lead to its degradation.

Studies have identified several genes associated with MMAF, amongst these *DNAH1* mutations are the most common, with mutations in this gene described in one-third to one-half of patients with MMAF [3, 5, 7]. DNAH1 is part of the inner dynein arm of the ciliary axoneme, and its mutation leads to serious disorders of the axial filament [3]. Previous studies have reported a large number of homozygous mutations in *DNAH*1 [3, 7]. However, compound heterozygous mutations, which may also result in the loss of protein function, account for a low proportion of these mutations. In our study, complex heterozygous mutations in *DNAH1* accounted for a higher proportion (62.5%, 5/8) of the sterile patients than previously reported. This may be due to the non-random collection method used in the recruitment of this study, sporadic sterile patients from non-consanguineous families with complex heterozygous mutations are at a disadvantage when evaluating underlying genetic predispositions to various diseases. Consanguineous families are more likely to give birth to patients with homozygous mutations, which are more easily identified and evaluated making them a more attractive prospect for early studies [22-24, 41-43]. If all MMAF patients undergo WES, more complex heterozygous mutations in *DNAH1* will be identified.

Inner dynein arms are an important dynamic source of sperm motility and are organised by seven molecular complexes arranged in 3-2-2 groups. The groups are composed of three different types of inner arms: IDA1, IDA2, and IDA3 [3] and DNAH1 is a critical component of IDA3. This implies that deficiencies in DNAH1 may result in a failure to provide an anchor site for radial spoke 3, which results in reduced attachment of the two central singlet microtubules [6]. *Mdhc7* (a *DNAH1* homologue) knockout mice exhibit significantly reduced progressive motility of spermatozoa, resulting in *Mdhc7*-deficient spermatozoa failing to move to the oviduct [44]. In the sperm of *Mdhc7*$^{-/-}$ mice, a visible two "heads" change occurs in IDA3 resulting from the loss of a C-terminal (globular) domain [45]. The three-dimensional movement of *Mdhc7*-deficient spermatozoa was normal; however, the maximum velocity and amplitude vibration decreased significantly [46]. No obvious ultrastructural defects were observed in the mitochondrial sheath or axonemal structure of *Mdhc7*-deficient spermatozoa [44]. In contrast, our results show that most of the sperm from patients with mutations in *DNAH1* had structural defects in the mitochondrial sheath and axonemal structure, indicating the crucial role of *DNAH1* in IDAs and sperm flagellar function in humans. Previous studies have also shown that mutations in *DNAH1* impair the ultrastructure of spermatozoa [3, 6, 7], which further confirms the critical action of *DNAH1* in human sperm flagella.

Primary ciliary dyskinesia (PCD [MIM:244400]) is a rare autosomal-recessive disease characterised by chronic airway infections with bronchitis and rhinosinusitis and/or associated situs inversus [47]. PCD may be incorrectly diagnosed or eliminated due to inexperience with diagnostic testing methods [38]. Following the publication of guidelines for the diagnosis of PCD by the American Thoracic Society and European Respiratory Society [48, 49], the accuracy of PCD diagnosis is gradually improving. However, milder PCD phenotypes may not be accurately diagnosed. In previous reports, MMAF patients with *DNAH1* mutations were not accompanied by a typical PCD phenotype [3, 5-7]. A reasonable explanation is that DNAH1 is mainly expressed in the flagella [3]. Mutations in *DNAH17* (MIM: 610063), which is specifically expressed in spermatozoa, only causes male asthenozoospermia and MMAF and not PCD [28]. These results suggest that genes expressed primarily in the flagella are likely to affect the function of sperm flagella but have limited impact on the cilia. Homozygous missense mutations *DNAH1* have been described in female PCD patients [50]; suggesting that MMAF patients with *DNAH1* mutations should be carefully screened for milder PCD phenotypes. None of our eight MMAF patients with *DNAH1* mutations exhibited any typical PCD symptoms; however, follow-up medical examinations of MMAF patients with *DNAH1* mutations are necessary to determine whether PCD symptoms appear at a later stage.

It has been reported that ICSI can be used to address infertility in MMAF patients with *DNAH1* mutations [31]. Here, three of our six MMAF *DNAH1* patients joined the ICSI treatment program and their wives successfully conceived. The families of the three patients who accepted the ICSI were financially able to afford the treatment, and were allowed to provide proper consent for all of the procedures. The blastocysts from each of the three couples met the transplant criteria underwent a complete ICSI treatment program. The embryos of these three patients did not develop very well on days 5-6; however, they still met our transplantation standards. After informing the patients of the details and advantages and disadvantages, they elected to continue with the process. Fortunately, the wives of all three patients were able to conceive. We found that embryonic dysplasia might be caused by several factors. Although the sperm quality of the patients is one of the factors, the age of the wives of the patients may also impact the quality of the embryos, making assisted reproduction a more complex process in general. The other three patients rejected the ICSI for various private reasons and were not included in our report.

Overall, the eggs from the wives of the three patients were successfully fertilised using ICSI, which suggests that these mutations did not affect the chromosomes of the sperm head despite the fact that the *DNAH1* mutations seriously disrupt the morphology of the sperm from MMAF patients. However, our ICSI attempts with MMAF patients who have mutations in other genes such as *CEP135* or *SPEF2* [18, 35], did not produce the desired result. Some investigations into MMAF patients and knockout animal models do not assess the effect of the pathogenic mutations on reproductive outcomes limiting our understanding of their impact [17, 36]. This finding indicates the potentially important role of using WES during ICSI evaluations in improving the treatment outcomes for MMAF patients.

Conclusions

We identified six novel biallelic mutations in *DNAH1* from 19 patients with MMAF. Our findings suggest that compound heterozygous mutations in *DNAH1* play an important role in the occurrence of MMAF. Our study provides a theoretical basis for the clinical diagnosis and treatment of male infertility caused by MMAF.

Abbreviations

MMAF: Multiple morphological anomalies of the sperm flagella; TEM: transmission electron microscopy; WES: whole-exome sequencing; ICSI: intracytoplasmic sperm injection; NGS: Next-generation sequencing; PCD: Primary ciliary dyskinesia; PB: Phosphate buffer; PBS: Phosphate-buffered saline;

PFA: Paraformaldehyde; ODF: outer dense fibre; DMT: doublet microtubules; NMD: nonsense-mediated mRNA decay.

Declarations

Acknowledgments

The authors would like to sincerely thank all the patients and donors for their interest and co-operation.

Ethics approval and consent to participate

This study was approved by the Ethics Committee of the Affiliated Yantai Yuhuangding Hospital of Qingdao University. Written informed consent forms were obtained from all subjects.

Consent for publication

The patients gave written consent for publication.

Conflict of interest

The authors have no conflicts of interest to declare.

Funding

This work was supported by the following grants: The Medicine and Health Science Technology Development Project of Shandong Province (Grant no. 2016WS0704), Natural Science Foundation of Shandong Province (Grant no. ZR2017LH012), the General Program of National Natural Science Foundation of China (Grant no. 81871200), the open project of NHC Key Laboratory of Male Reproduction and Genetics (No. KF201704; NO. KF201807), Guangzhou Science and Technology Plan Project (201707010394), and The Professor and Academic Development Fund from the Fujian Medical University (NO: JS15010).

Availability of data and materials

The datasets used and/or analysed during this study are available from the corresponding author upon reasonable request.

References

1. Krausz, C. and A. Riera-Escamilla, *Genetics of male infertility.* Nat Rev Urol, 2018. **15**(6): p. 369-384.
2. Esteves, S.C., *A clinical appraisal of the genetic basis in unexplained male infertility.* J Hum Reprod Sci, 2013. **6**(3): p. 176-82.
3. Ben Khelifa, M., et al., *Mutations in DNAH1, which encodes an inner arm heavy chain dynein, lead to male infertility from multiple morphological abnormalities of the sperm flagella.* Am J Hum Genet, 2014. **94**(1): p. 95-104.
4. Bamshad, M.J., et al., *Exome sequencing as a tool for Mendelian disease gene discovery.* Nat Rev Genet, 2011. **12**(11): p. 745-55.
5. Amiri-Yekta, A., et al., *Whole-exome sequencing of familial cases of multiple morphological abnormalities of the sperm flagella (MMAF) reveals new DNAH1 mutations.* Hum Reprod, 2016. **31**(12): p. 2872-2880.
6. Sha, Y., et al., *DNAH1 gene mutations and their potential association with dysplasia of the sperm fibrous sheath and infertility in the Han Chinese population.* Fertil Steril, 2017. **107**(6): p. 1312-1318 e2.
7. Wang, X., et al., *Homozygous DNAH1 frameshift mutation causes multiple morphological anomalies of the sperm flagella in Chinese.* Clin Genet, 2017. **91**(2): p. 313-321.
8. Li, Y., et al., *DNAH2 is a novel candidate gene associated with multiple morphological abnormalities of the sperm flagella.* Clin Genet, 2019. **95**(5): p. 590-600.
9. Yang, Y., et al., *Loss-of-function mutation in DNAH8 induces asthenoteratospermia associated with multiple morphological abnormalities of the sperm flagella.* Clin Genet, 2020.
10. Liu, C., et al., *Bi-allelic DNAH8 Variants Lead to Multiple Morphological Abnormalities of the Sperm Flagella and Primary Male Infertility.* Am J Hum Genet, 2020. **107**(2): p. 330-341.
11. Baccetti, B., et al., *Gene deletions in an infertile man with sperm fibrous sheath dysplasia.* Hum Reprod, 2005. **20**(10): p. 2790-4.
12. Merveille, A.C., et al., *CCDC39 is required for assembly of inner dynein arms and the dynein regulatory complex and for normal ciliary motility in humans and dogs.* Nat Genet, 2011. **43**(1): p. 72-8.
13. Coutton, C., et al., *Mutations in CFAP43 and CFAP44 cause male infertility and flagellum defects in Trypanosoma and human.* Nat Commun, 2018. **9**(1): p. 686.
14. Sha, Y.W., et al., *Patients with multiple morphological abnormalities of the sperm flagella harbouring CFAP44 or CFAP43 mutations have a good pregnancy outcome following intracytoplasmic sperm injection.* Andrologia, 2018: p. e13151.
15. Tang, S., et al., *Biallelic Mutations in CFAP43 and CFAP44 Cause Male Infertility with Multiple Morphological Abnormalities of the Sperm Flagella.* Am J Hum Genet, 2017. **100**(6): p. 854-864.
16. He, X., et al., *Bi-allelic Loss-of-function Variants in CFAP58 Cause Flagellar Axoneme and Mitochondrial Sheath Defects and Asthenoteratozoospermia in Humans and Mice.* Am J Hum Genet, 2020. **107**(3): p. 514-526.

17. Dong, F.N., et al., *Absence of CFAP69 Causes Male Infertility due to Multiple Morphological Abnormalities of the Flagella in Human and Mouse.* Am J Hum Genet, 2018. **102**(4): p. 636-648.
18. Sha, Y.W., et al., *A homozygous CEP135 mutation is associated with multiple morphological abnormalities of the sperm flagella (MMAF).* Gene, 2017. **633**: p. 48-53.
19. Martinez, G., et al., *Whole-exome sequencing identifies mutations in FSIP2 as a recurrent cause of multiple morphological abnormalities of the sperm flagella.* Hum Reprod, 2018. **33**(10): p. 1973-1984.
20. Li, W., et al., *Biallelic mutations of CFAP251 cause sperm flagellar defects and human male infertility.* J Hum Genet, 2018.
21. Auguste, Y., et al., *Loss of Calmodulin- and Radial-Spoke-Associated Complex Protein CFAP251 Leads to Immotile Spermatozoa Lacking Mitochondria and Infertility in Men.* Am J Hum Genet, 2018. **103**(3): p. 413-420.
22. Kherraf, Z.E., et al., *A Homozygous Ancestral SVA-Insertion-Mediated Deletion in WDR66 Induces Multiple Morphological Abnormalities of the Sperm Flagellum and Male Infertility.* Am J Hum Genet, 2018. **103**(3): p. 400-412.
23. Coutton, C., et al., *Bi-allelic Mutations in ARMC2 Lead to Severe Astheno-Teratozoospermia Due to Sperm Flagellum Malformations in Humans and Mice.* Am J Hum Genet, 2019. **104**(2): p. 331-340.
24. Liu, C., et al., *Homozygous mutations in SPEF2 induce multiple morphological abnormalities of the sperm flagella and male infertility.* J Med Genet, 2019.
25. Liu, W., et al., *Loss-of-function mutations in SPEF2 cause multiple morphological abnormalities of the sperm flagella (MMAF).* J Med Genet, 2019.
26. Sha, Y., et al., *Biallelic mutations in Sperm flagellum 2 cause human multiple morphological abnormalities of the sperm flagella (MMAF) phenotype.* Clin Genet, 2019.
27. Zhang, B., et al., *A DNAH17 missense variant causes flagella destabilization and asthenozoospermia.* J Exp Med, 2019.
28. Whitfield, M., et al., *Mutations in DNAH17, Encoding a Sperm-Specific Axonemal Outer Dynein Arm Heavy Chain, Cause Isolated Male Infertility Due to Asthenozoospermia.* Am J Hum Genet, 2019. **105**(1): p. 198-212.
29. Wang, W.L., C.F. Tu, and Y.Q. Tan, *Insight on multiple morphological abnormalities of sperm flagella in male infertility: what is new?* Asian J Androl, 2020. **22**(3): p. 236-245.
30. Sha, Y., et al., *DNAH17 is associated with asthenozoospermia and multiple morphological abnormalities of sperm flagella.* Ann Hum Genet, 2020. **84**(3): p. 271-279.
31. Wambergue, C., et al., *Patients with multiple morphological abnormalities of the sperm flagella due to DNAH1 mutations have a good prognosis following intracytoplasmic sperm injection.* Hum Reprod, 2016. **31**(6): p. 1164-72.
32. Sha, Y.W., et al., *Patients with multiple morphological abnormalities of the sperm flagella harbouring CFAP44 or CFAP43 mutations have a good pregnancy outcome following intracytoplasmic sperm injection.* Andrologia, 2019. **51**(1): p. e13151.
33. Sha, Y., et al., *Biallelic mutations of CFAP74 may cause human primary ciliary dyskinesia and MMAF phenotype.* J Hum Genet, 2020.
34. Ni, X., et al., *A novel homozygous mutation in WDR19 induces disorganization of microtubules in sperm flagella and nonsyndromic asthenoteratospermia.* J Assist Reprod Genet, 2020. **37**(6): p. 1431-1439.
35. Liu, W., et al., *Loss-of-function mutations in SPEF2 cause multiple morphological abnormalities of the sperm flagella (MMAF).* J Med Genet, 2019. **56**(10): p. 678-684.
36. Li, W., et al., *Biallelic mutations in CFAP65 cause male infertility with multiple morphological abnormalities of the sperm flagella in humans and mice.* J Med Genet, 2020. **57**(2): p. 89-95.
37. Yang, S.M., et al., *Morphological characteristics and initial genetic study of multiple morphological anomalies of the flagella in China.* Asian J Androl, 2015. **17**(3): p. 513-5.
38. Shapiro, A.J., et al., *Diagnosis, monitoring, and treatment of primary ciliary dyskinesia: PCD foundation consensus recommendations based on state of the art review.* Pediatr Pulmonol, 2016. **51**(2): p. 115-32.
39. Sha, Y.W., et al., *TSGA10 is a novel candidate gene associated with acephalic spermatozoa.* Clin Genet, 2018. **93**(4): p. 776-783.
40. Sha, Y.W., et al., *First successful pregnancy outcome after intracytoplasmic sperm injection with short-tailed sperm from an infertile Han Chinese man.* Asian J Androl, 2017. **19**(5): p. 613-614.
41. Zhang, X., et al., *A novel homozygous CFAP65 mutation in humans causes male infertility with multiple morphological abnormalities of the sperm flagella.* Clin Genet, 2019.
42. Wu, H., et al., *NovelCFAP43 andCFAP44 mutations cause male infertility with multiple morphological abnormalities of the sperm flagella (MMAF).* Reprod Biomed Online, 2019. **38**(5): p. 769-778.
43. He, X., et al., *Novel homozygous CFAP69 mutations in humans and mice cause severe asthenoteratospermia with multiple morphological abnormalities of the sperm flagella.* J Med Genet, 2019. **56**(2): p. 96-103.
44. Neesen, J., et al., *Disruption of an inner arm dynein heavy chain gene results in asthenozoospermia and reduced ciliary beat frequency.* Hum Mol Genet, 2001. **10**(11): p. 1117-28.
45. Vernon, G.G., J. Neesen, and D.M. Woolley, *Further studies on knockout mice lacking a functional dynein heavy chain (MDHC7). 1. Evidence for a structural deficit in the axoneme.* Cell Motil Cytoskeleton, 2005. **61**(2): p. 65-73.
46. Woolley, D.M., J. Neesen, and G.G. Vernon, *Further studies on knockout mice lacking a functional dynein heavy chain (MDHC7). 2. A developmental explanation for the asthenozoospermia.* Cell Motil Cytoskeleton, 2005. **61**(2): p. 74-82.
47. Butterfield, R., *Primary Ciliary Dyskinesia.* Pediatr Rev, 2017. **38**(3): p. 145-146.

48. Shapiro, A.J., et al., *Diagnosis of Primary Ciliary Dyskinesia. An Official American Thoracic Society Clinical Practice Guideline.* Am J Respir Crit Care Med, 2018. **197**(12): p. e24-e39.

49. Dalrymple, R.A. and P. Kenia, *European Respiratory Society guidelines for the diagnosis of primary ciliary dyskinesia: a guideline review.* Arch Dis Child Educ Pract Ed, 2019. **104**(5): p. 265-269.

50. Imtiaz, F., et al., *Variation in DNAH1 may contribute to primary ciliary dyskinesia.* BMC Med Genet, 2015. **16**: p. 14.

Tables

Table 1: Semen parameters of the patients with MMAF.

Patient	Semen volume (ml)	Sperm concentration (10^6/ml)	Sperm progressive motility (%)	Sperm motility (%)	Percentage of normal sperm (%)	Flagella (%)					
						Normal	Absent	Short	Coiled	Angulation	Irregular width
P002	2.2	16.9	0	0	0.5	3	10	47	4	5	38
P005	2.5	23.5	1.5	2.3	0.5	8	14	35	6	8	43
P008	1.8	25.3	0	0	1.0	10	12	43	8	6	47
P011	3.0	3.5	0	0	0	0	18	50	11	6	35
P015	2.6	14.0	0	0	0.5	5	16	62	5	10	33
P017	3.2	17.65	1.2	5.6	0.5	2	20	55	10	8	26

TABLE 2: In silico analysis of the pathogenic for the *DNAH1* mutations

Patient	Mutation	Amino acid change	Polyphen-2_HDIV[a]	Polyphen-2_HVAR[b]	LRT[c]	Mutation Taster[d]	FATHMM_MKL[e]	GenoCanyon[f]	ClinPred[g]
P002	g.52400764G>C	p.Ala1876Pro	Probably damaging (0.992)	Probably damaging (0.962)	Deleterious (0)	Disease causing(1)	Damaging (0.998)	Damaging (1)	Pathoge (0.97238
	g.52431052G>A	p.Asp3927Asn	Probably damaging (1)	Probably damaging (0.996)	Deleterious (0)	Disease causing (0.999)	Damaging (0.894)	Damaging (1)	Benign (0.12306
P005	g.52414014C>A	p.Gln2491Lys	Benign (0)	Benign (0)	Neutral (0.79)	Disease causing(1)	Tolerable (0.008)	Tolerable (0.915)	Benign (0.00724
	g.52423486C>T	p.Arg3169Cys	Probably damaging (1)	Probably damaging (1)	Deleterious (0)	Disease causing(1)	Damaging (0.984)	Damaging (1)	Pathoge (0.99982
P008	g.52417875G>C	3p21.1	NA	NA	NA	Disease causing(1)	Damaging (0.994)	Damaging (1)	NA
	g.52430998-52430999del	p.Pro3909fs	NA	NA	NA	NA	NA	NA	NA
P011	g.52390782C>G	p.Tyr1282X	NA	NA	Neutral (0.009)	Disease causing(1)	Tolerable (0.044)	Damaging (1)	NA
P015	g.52370722_52370723del	p.Thr2141fs	NA	NA	NA	NA	NA	NA	NA
	g.52375320C>T	p.Arg2356Trp	Probably damaging (1)	Probably damaging (1)	Deleterious (0)	Disease causing(1)	NA	NA	Pathoge (0.99689
P017	g.52417883G>A	p.Gly2720Arg	Probably damaging (1)	Probably damaging (0.996)	Deleterious (0)	Disease causing(1)	Damaging (0.992)	Damaging (1)	Pathoge (0.77313
	g.52432907A>T	p.Asp4044Val	Probably damaging (0.992)	Possibly damaging (0.886)	Deleterious (0)	Disease causing(1)	Damaging (0.988)	Damaging (1)	Pathoge (0.98646

a Polyphen-2_HDIV (http://genetics.bwh.harvard.edu/pph2/). Evaluating rare alleles at loci potentially involved in complex phenotypes, dense mapping of regions identified by genome-wide association studies, and analysis of natural selection from sequence data. The authors recommend calling "probably damaging" if the score is between 0.957 and 1, and "possibly damaging" if the score is between 0.453 and 0.956, and "benign" is the score is between 0 and 0.452.

b Polyphen-2_HVAR (http://genetics.bwh.harvard.edu/pph2/). Diagnostics of Mendelian diseases, which requires distinguishing mutations with drastic effects from all the remaining human variation, including abundant mildly deleterious alleles.The authors recommend calling "probably damaging" if the score is

between 0.909 and 1, and "possibly damaging" if the score is between 0.447 and 0.908, and "benign" is the score is between 0 and 0.446.

c LRT (http://www.genetics.wustl.edu/jflab/). The effect of variant on protein sequence. D: Deleterious; N: Neutral; U: Unknown

d Mutation Taster (http://www.mutationtaster.org/). The probability value is the probability of the prediction, that is, a value close to 1 indicates a high "security" of the prediction.

e FATHMM_MKL (http://fathmm.biocompute.org.uk/). The effect of variant on protein sequence. D: Deleterious; T: Tolerated

f ClinPred (https://sites.google.com/site/clinpred/). Efficient tool for identifying disease-relevant nonsynonymous single nucleotide variants.

TABLE 3: In silico analysis of the conservatism and frequency for the *DNAH1* mutations

Mutation	Amino acid change	GERP++[a]	phyloP[b]	phastCons[c]	SiPhy[d]	1000G_ALL[e]	ESP6500[f]	gnomAD[g]
g.52400764G>C	p.Ala1876Pro	Conserved (4.97)	Conserved (9.707)	Conserved (1)	Conserved (18.241)	NA	NA	0.0000081
g.52431052G>A	p.Asp3927Asn	Conserved (4.27)	Conserved (5.661)	Conserved (1)	Conserved (16.911)	NA	NA	0.0000353
g.52414014C>A	p.Gln2491Lys	Nonconserved (-4.76)	Nonconserved (0.021)	Nonconserved (0)	Nonconserved (10.405)	0.0002	NA	0.0001
g.52423486C>T	p.Arg3169Cys	Conserved (5.06)	Conserved (4.151)	Conserved (1)	Conserved (18.812)	0.0002	NA	0.0000167
g.52417875G>C	3p21.1	Conserved (4.19)	Conserved (8.097)	Conserved (1)	Conserved (16.726)	NA	NA	NA
g.52430998-52430999del	p.Pro3909fs	NA	NA	NA	NA	0.0014	0	0.0000983
g.52390782C>G	p.Tyr1282X	Nonconserved (-10.3)	Nonconserved (-3.347)	Nonconserved (0)	Nonconserved (9.627)	0	NA	0.0000085
g.52370722_52370723del	p.Thr2141fs	NA	NA	NA	NA	NA	NA	NA
g.52375320C>T	p.Arg2356Trp	Nonconserved (1.48)	Nonconserved (1.175)	Nonconserved (0.491)	Conserved (15.752)	NA	NA	0.0000081
g.52417883G>A	p.Gly2720Arg	Conserved (4.19)	Conserved (9.953)	Conserved (1)	Conserved (13.98)	0.000199681	NA	0.0001
g.52432907A>T	p.Asp4044Val	Conserved (4.34)	Conserved (7.095)	Conserved (1)	Conserved (16.726)	NA	NA	0.0000128

a GERP++ (http://mendel.stanford.edu/SidowLab/downloads/gerp/).

b phyloP (http://compgen.bscb.cornell.edu/phast/).

c phastCons (http://compgen.bscb.cornell.edu/phast/).

d SiPhy (http://portals.broadinstitute.org/genome_bio/siphy/).

E 1000G (https://www.internationalgenome.org/). Frequency of variation in total of 1000 Genomes database (A Deep Catalog of Human Genetic Variation).

f ESP6500 (https://esp.gs.washington.edu/drupal/). Frequency of variation in ESP6500 database.

d gnomAD (https://macarthurlab.org/2019/10/16/gnomad-v3-0/). Frequency of variation in gnomAD database.

Table 4: ICSI outcomes and pregnancy

Patient	Age of patient's wife	Collected oocytes	Injected oocytes	Embryos	Transferred embryos	Degenerate embryos	Frozen embryos	Clinical pregnancy	Delivery
P002	29	7	5	5	2	2	1	1	1
P008	35	11	8	7	2	2	3	1	1
P011	28	13	13	7	2	3	2	1	1

Figures

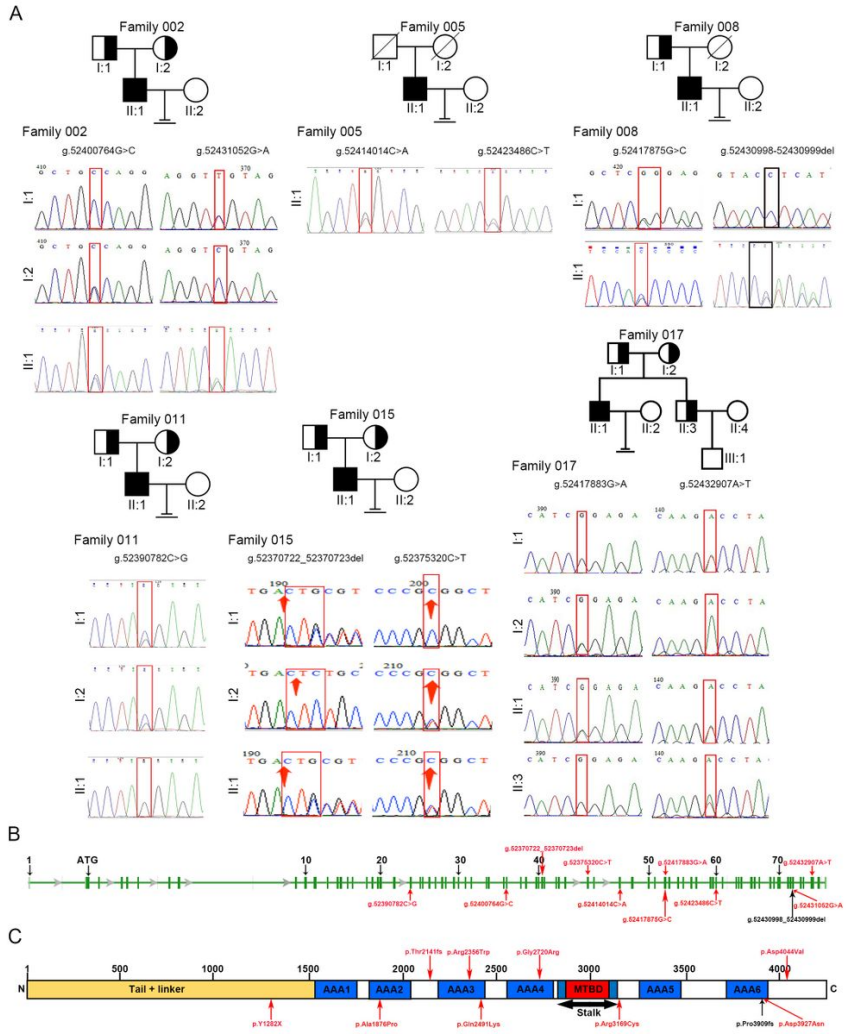

Figure 1

Ten novel DNAH1 mutation sites were identified in six sterile MMAF patients. (A) Sanger sequencing confirmed the DNAH1 mutations in both the patients and their parents. The rectangles indicate the mutation sites in each of the six sterile MMAF patients. The red rectangles identify each of the ten novel mutation sites. (B) Locations of the DNAH1 mutation sites the red arrows indicate the ten novel mutation sites and the green boxes indicate the exons. (C) Structural location of the DNAH1 mutations the red arrows indicate the location of the affected amino acids and the blue boxes indicate the six known AAA-ATPase domains (AAA 1 to 6). MTBD: microtubule-binding domain.

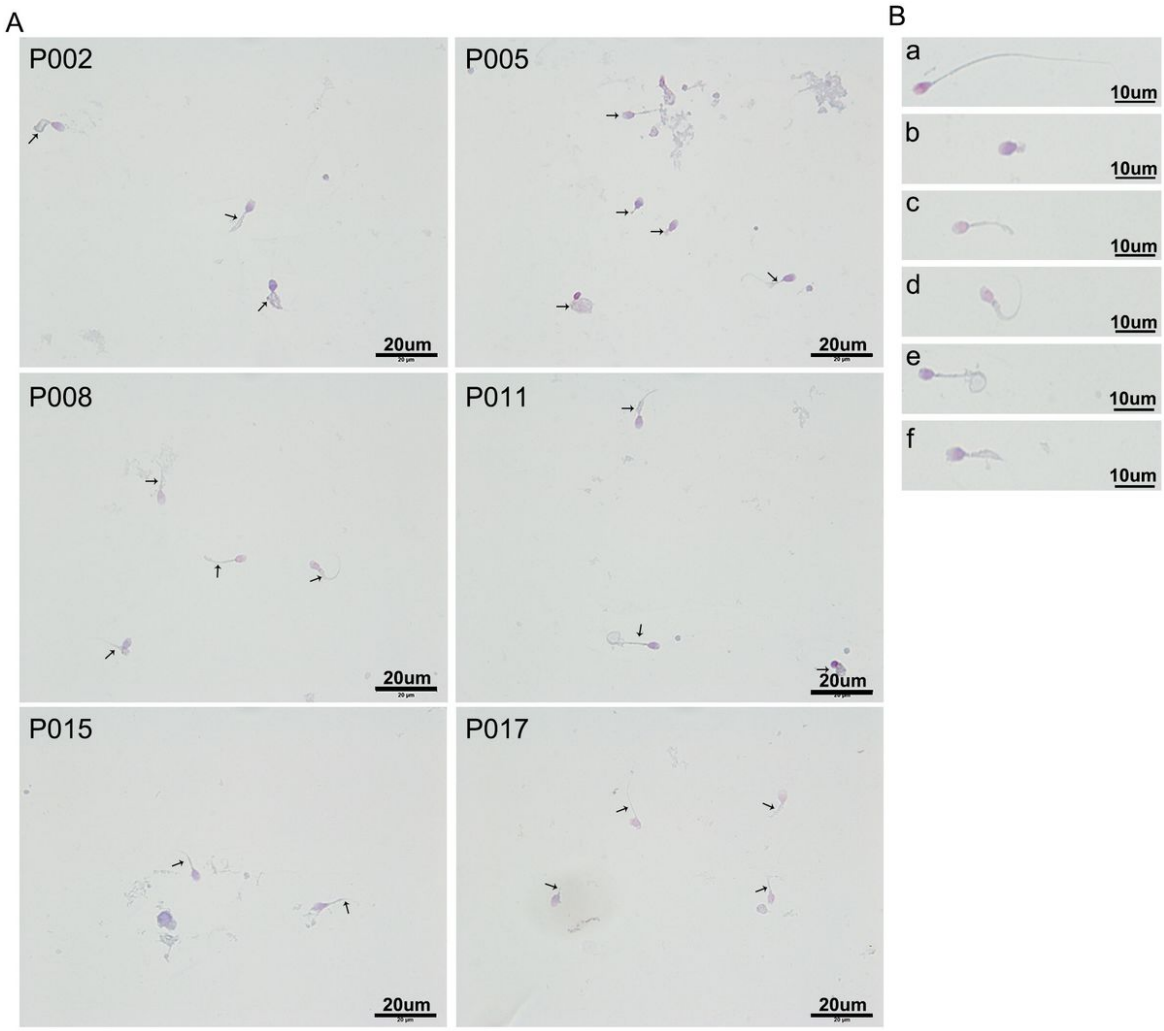

Figure 2

Morphological defects in the spermatozoa of MMAF patients with DNAH1 mutations. (A) Morphology of spermatozoa from the patients (P002, P005, P008, P011, P015, and P017) was assessed using Papanicolaou staining, which revealed multiple morphological abnormalities in the flagella (indicated by black arrows). (B) Typical morphology of the spermatozoa from the control subject and patients. a: Normal spermatozoa from control subjects. b-f: Typical morphology of the sperm of the patients, including absent (b), short (c), bent (d), coiled (e), and/or irregular (f) flagella. Multiple images were taken, and representative images are presented here. Scale bar: A: 20 μm; B: 10 μm.

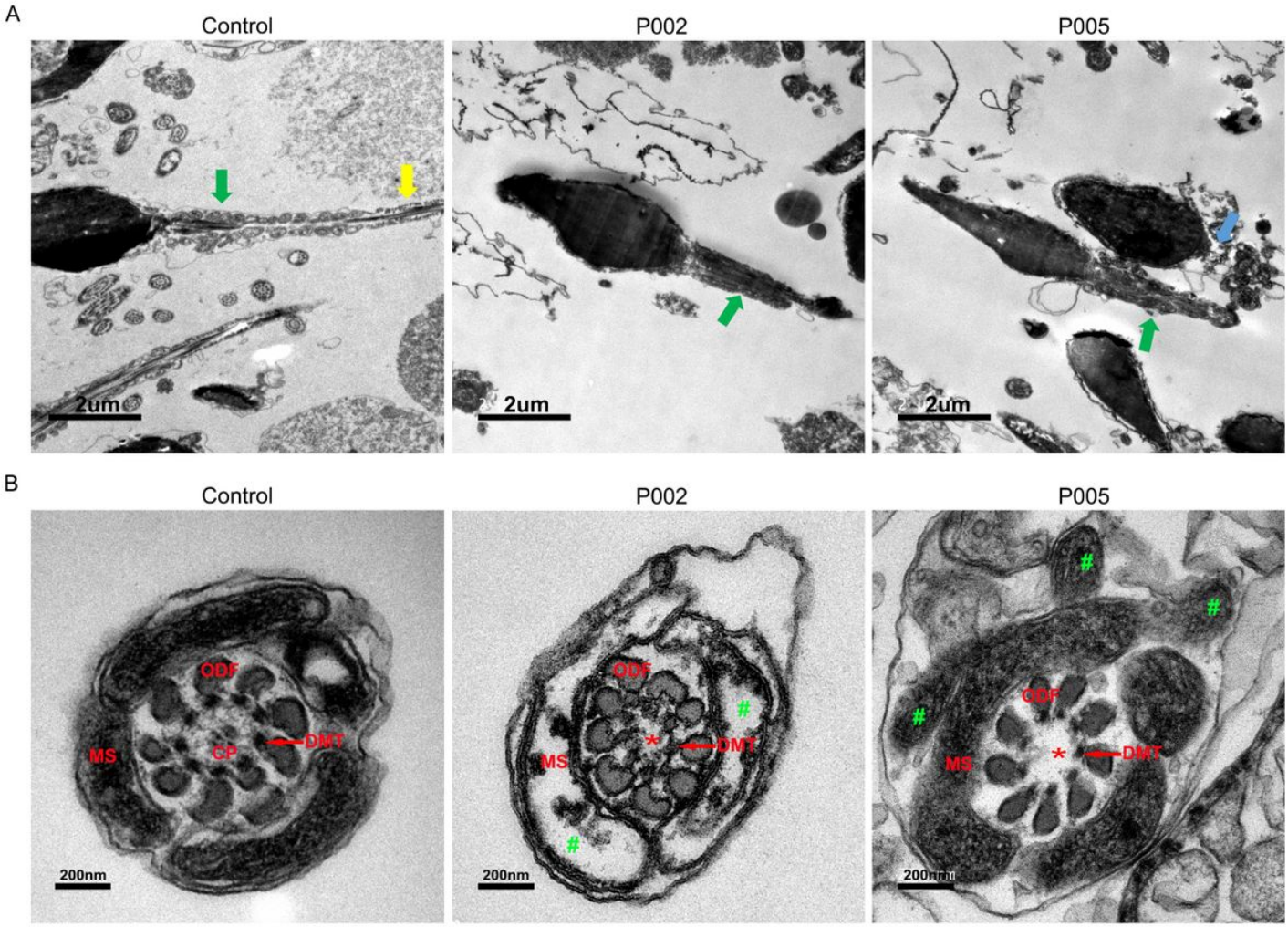

Figure 3

Spermatozoa ultrastructure defects in patients with MMAF. (A) Longitudinal sections of the spermatozoa from the control subject and patients. The midpiece of the spermatozoa from the control subject is indicated by the green arrow, and the principal piece is indicated by the yellow arrow (left). The midpiece of the short-flagella spermatozoa from P002 (middle) and the midpiece of the short-flagella spermatozoa from P005 are indicated by the green arrows, while those with absent flagella are indicated by the blue arrow (right). (B) Cross-sections of the midpiece of the spermatozoa from the control subject and patients are shown. Spermatozoa from the control subject had typical “9+2” microtubule structures, including nine ODFs, nine DMTs, and a pair of central microtubules (left). The central pairs of the spermatozoa from P002 were absent (indicated by red *), and the mitochondrial sheath was defective (indicated by green #) (middle). Spermatozoa from P005 presented without central pairs (indicated by red *) and the mitochondrial sheath was disordered (indicated by green #) (left). Multiple images were taken, and representative images are presented. Scale bar: A: 2 μm; B: 200 μm.

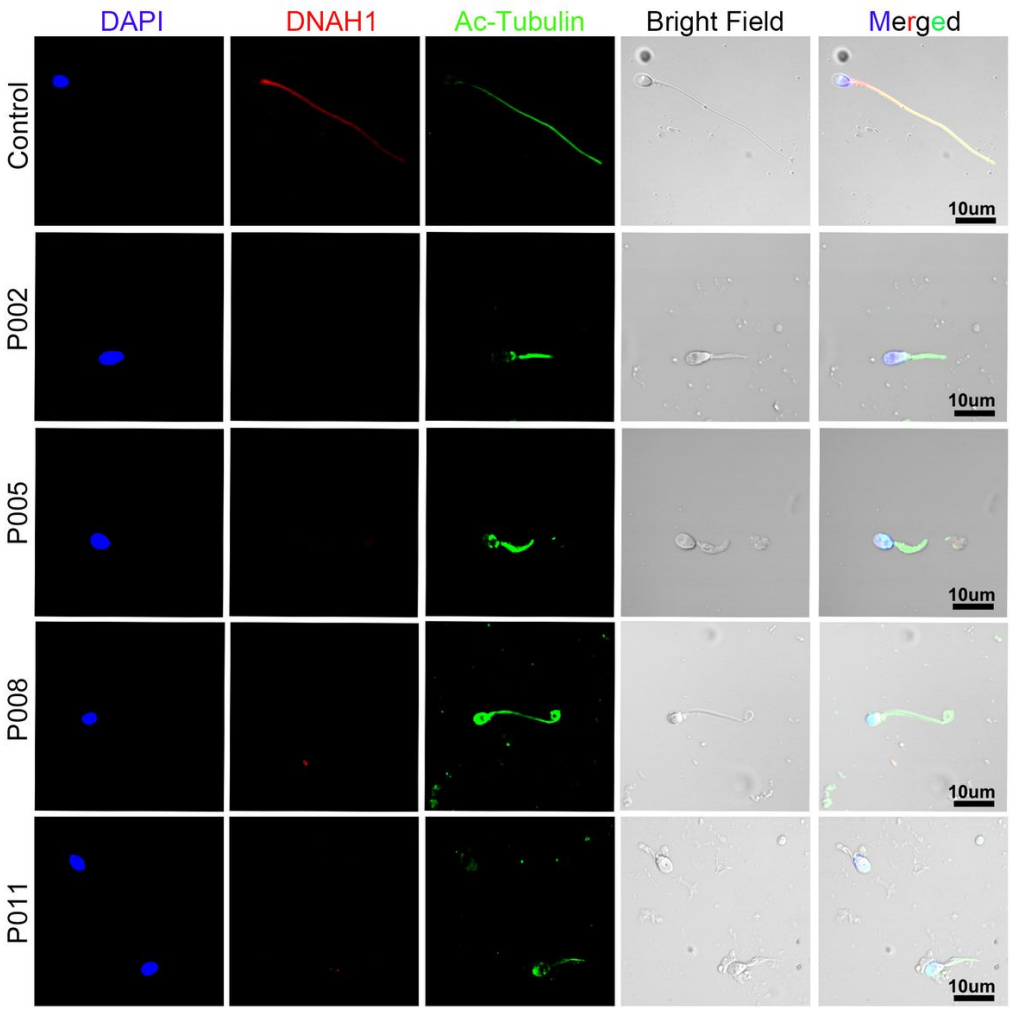

Figure 4

DNAH1 expression in the control subjects and patients. Immunofluorescence staining was performed to evaluate DNAH1 (red) expression in spermatozoa samples from both the control samples and the patients with DNAH1 mutations. Ac-tubulin (Green) was used to identify the flagella and DAPI (Blue) was used to stain the nucleus of the spermatozoa. Multiple images were taken, and representative images are presented. Scale bar: 10 μm.

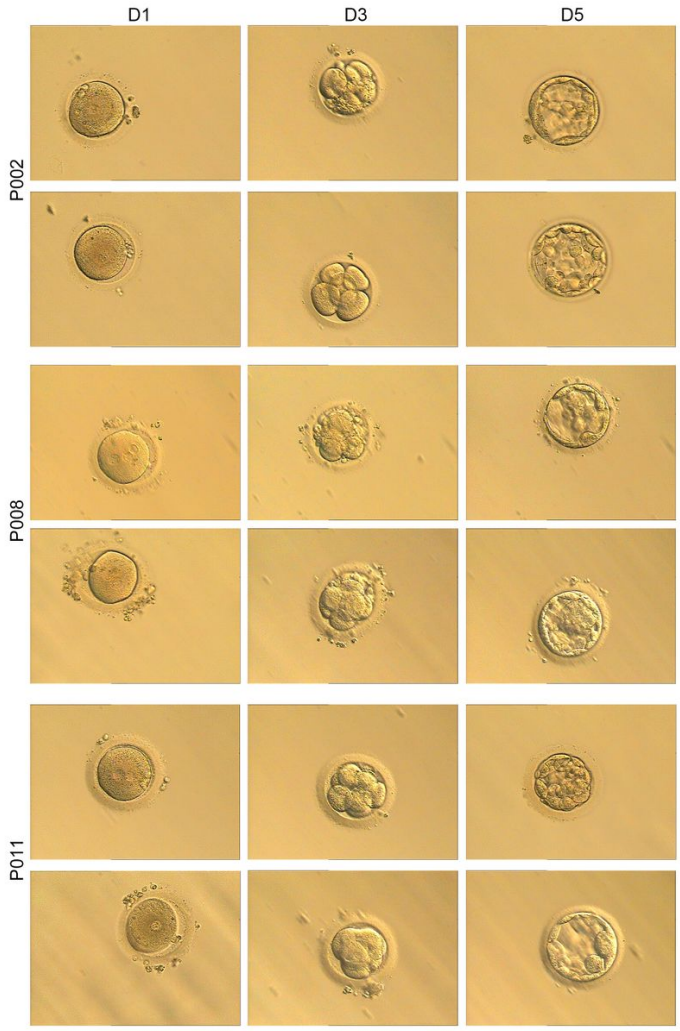

Figure 5

Embryogenesis in the implanted embryos. The embryogenesis of zygotes from patients with DNAH1 mutations (P002, P008, and P011) at D1, D3, and D5 is shown.

Supplementary Files

This is a list of supplementary files associated with this preprint. Click to download.

- SupplementaryFig.1.tif
- SupplementaryTable.docx